

Dependence of R fluorescence lines of rubies on Cr³⁺ concentration at various temperatures, with implications for pressure calibrations in experimental apparatus

RONG GAO^{1,2,†}, HEPING LI^{1,*} AND JINGTAI ZHAO^{2,3}

¹Key Laboratory of High-temperature and High-Pressure Study of the Earth's Interior, Institute of Geochemistry, Chinese Academy of Sciences, Guiyang, Guizhou Province, 550002, P.R. China

²Key Laboratory of Transparent Opto-Functional Inorganic Materials, Shanghai Institute of Ceramics, Chinese Academy of Sciences, Shanghai 200050, P.R. China

³School of Materials Science and Engineering, Shanghai University, Shanghai 200072, P.R. China

ABSTRACT

The R fluorescence lines of rubies that contain 0.022, 0.068, 0.211, 0.279, 0.556, 1.221, and 1.676 wt% of Cr₂O₃ were measured at temperatures of 100–600 K and at atmospheric pressure. The R₁ line wavenumbers of all of the ruby samples shifted linearly as the temperature increased from 298 to 600 K at atmospheric pressure, and the temperature dependence increased from -0.157 ± 0.001 cm⁻¹/K to -0.149 ± 0.001 cm⁻¹/K as the Cr₂O₃ content in the rubies increased from 0.022 to 1.676 wt%, which suggests a significant dependence on Cr³⁺ concentration. At room temperature and atmospheric pressure, the full-width at half maximum (FWHM) of the peak height of the R lines also appears to be linearly related to the Cr³⁺ concentration. The relative intensity ratios of the R₂ to R₁ lines (I_2/I_1) of ruby samples with different Cr³⁺ concentrations show several non-linear variations with temperature from 100 to 600 K, and the maximum values, $(I_2/I_1)_{\max}$, occur near room temperature. The effect of Cr³⁺ doping on the temperature dependence of the R line wavenumbers should be considered when rubies are used to calibrate the pressure or temperature in high-pressure and high-temperature experiments.

Keywords: R fluorescence lines, pressure calibration, temperature correction, ruby, Cr₂O₃ content

INTRODUCTION

Rubies are important photonic crystals, and their R fluorescence lines vary with pressure and temperature. The variations of the wavenumbers of R lines with pressure are commonly used to calibrate the pressure in diamond-anvil cells (DACs) (Forman et al. 1972; Mao et al. 1986). The variations in the intensity of R lines have also been used to calibrate temperature in scientific research (Weinstein 1986). Because the R lines are caused by the excitation of the 3d electrons in their ground states and their subsequent de-excitation from their excitation states and because there are inevitable interactions between Cr³⁺ in the ruby lattice, the concentration of Cr³⁺ in rubies may affect both the pressure and temperature dependence of the R lines at high temperature and high pressure conditions. Therefore, the quantitative investigation of the effect of Cr³⁺ doping on the pressure and temperature behaviors of R lines is important for the accuracy of pressure and temperature calibrations in simultaneous high-pressure and high-temperature DAC experiments, which are often used to study the Earth's interior (Chou 2003) and in other high-pressure sciences, such as high-pressure physics, chemistry, life science, and material science.

Variations in the peak position and the width and intensity of the ruby R₁ line as a function of temperature have been analyzed in several studies, but the results vary widely (Kokhanenko and

Antipov 1969; Barnett et al. 1973; Yamaoka et al. 1980; Wunder and Schoen 1981; Ragan et al. 1992; Yen and Nicol 1992; Goncharov et al. 2005). For example, Ragan et al. (1992) determined a temperature dependence of 0.158 cm⁻¹/K from 390–600 K for the R₁ line wavenumber, which was approximately 11% greater than the value of 0.0068 nm/K (equivalent to approximately 0.141 cm⁻¹/K) that was reported by Barnett et al. (1973) and Yamaoka et al. (1980). When calibrating the pressure or temperature in a heating DAC experiment from 300 to 600 K using the R₁ line, this difference would lead to a maximum temperature discrepancy of 34 K or a maximum pressure discrepancy of 675 MPa. In fact, the reference contents of Cr₂O₃ in rubies used by previous researchers (0.062, 0.5, ~1, and 2 wt% Cr₂O₃ by Yen and Nicol 1992; Barnett et al. 1973; Yamaoka et al. 1980; and Wunder and Schoen 1981, respectively) were not the same. Does the concentration of Cr³⁺ contribute to this discrepancy? This study attempts to answer this question by measuring the temperature variations of the R lines of rubies with varying Cr³⁺ concentrations at atmospheric pressure.

EXPERIMENTAL METHODS

Pink to blood red synthetic rubies were cut into disks that were ~0.5 mm in diameter and ~0.2 mm thick and then polished. The concentrations of Cr³⁺ in the rubies were measured using an EPMA-1600 type electron probe (beam size 10 μm) with wavelength-dispersive spectroscopy (WDS) mode and an atomic absorption spectrophotometer (AAS). Three to five spots were measured in each sample. The average values are listed in Table 1. The Cr₂O₃ contents in rubies were from 0.022 to 1.676 wt%.

In the fluorescence measurement experiments that were conducted at high temperatures and atmospheric pressure, the samples were heated and cooled in a

* E-mail: liheping@vip.gyig.ac.cn

† Present address: Shanghai Institute of Ceramics, Chinese Academy of Sciences, Shanghai, 200050, P.R. China.

Linkam heating stage with a liquid nitrogen flowing system. The temperature was increased by 15 K/min and measured with a thermocouple. The precision of the temperature measurements was ± 0.1 K. The fluorescence spectra of the samples were excited and recorded using a confocal Renishaw inVia Micro-Raman Spectroscopy system. The system uses a 514.5 nm laser beam, which is produced by a Spectra Physics 2017 2 W argon ion laser and is focused on a spot on the sample by a Leica microscope system, as the excitation light source of the fluorescence. A high-resolution white light image of the samples that covers the sampling spot can be displayed on a screen of the Leica microscope system. In our experiments, (1) the silicon 520 cm⁻¹ peak calibration was performed before the fluorescence spectra were collected, and the accuracy of the spectrum collection was up to ± 0.01 cm⁻¹; (2) the excitation laser powers ranged from 0.0002 to 0.05 mW; (3) a 20 \times Olympus ULWD objective was used for the Leica microscope system, so the excitation laser beam was focused onto a ~ 2 μ m diameter spot; and (4) all of the fluorescence spectra were collected near the spots where the electron microprobe measurements were made.

In the fluorescence measurement experiments that were conducted at high pressures and room temperature, the fluorescence spectra of each ruby sample were measured at pressures of 0–2.0 GPa using the fluorescence measurement system described above and a DAC. The anvil culets of the DAC were approximately 500 μ m in diameter. The T301 stainless steel gasket (300 μ m thick with a sample hole that was 280 μ m in diameter) and a mixture of methanol, ethanol, and water at 16:3:1 volume proportions were used as the sample chamber and pressure medium, respectively, and could maintain a hydrostatic pressures up to ~ 10.5 GPa at room temperature (Angel et al. 2007). The pressures in the cell were measured using the wavenumber shift of the R₁ fluorescence peak of ruby no. 5, which contained 0.556 wt% of Cr₂O₃. The uncertainty of this technique below 2.0 GPa was estimated to be ± 50 MPa (Schmidt and Ziemann 2000).

The wavenumber of each fluorescence peak was obtained using the peak fitting program of the WIRE 3.1 software package from Renishaw Co. The R₁ line generally had a Lorentzian-type shape, but the R₂ line at high temperature was fit better by a Voigt type line that included Gaussian and Lorentzian components, and the Gaussian proportion increased with increasing temperature and Cr³⁺ concentration in the ruby samples.

Finally, the electron densities of state (DOS) of the Cr³⁺ 3d band in the rubies at ambient pressure and 10 GPa were calculated by the first principle calculation method using the crystal structure data of Al_{1.98}Cr_{0.02}O₃, Al_{1.92}Cr_{0.08}O₃, Al_{1.896}Cr_{0.104}O₃, and Al_{1.54}Cr_{0.46}O₃ in the ICSD database. The calculations used the Generalized Gradient Approximation (GGA) method, the PBE exchange-correlation function (Perdew et al. 1996) and ultra-soft potentials, and a 3 \times 3 \times 3 k-point mesh and 300 eV cut-off energy were chosen.

RESULTS AND DISCUSSION

Fluorescence peaks and their positions

The fluorescence spectra and the Raman spectra of the ruby samples with the lowest and highest Cr₂O₃ contents used in this study are shown in Figure 1. In addition to the well-known R₁ and R₂ peaks, several new peaks were present in the fluorescence spectra of rubies with Cr³⁺ concentrations greater than 0.5 wt%, and the relative intensities of the new peaks increased with increasing Cr₂O₃ content. A high Cr³⁺ concentration would lead to

strong Cr³⁺-Cr³⁺ interactions, which change the electron structure of the Cr³⁺. Thus, the new peaks might be attributed to Cr³⁺-Cr³⁺ interactions in the ruby lattice because the fluorescence spectra of rubies originate from the excitation of the 3d electrons in their ground states and their subsequent de-excitation from their respective excitation states. However, because the Raman spectra were similar, the increase of Cr³⁺ concentration likely does not cause the separation of a new phase from the ruby matrix.

Significantly varying shifts of the wavenumber positions of the R lines with Cr³⁺ concentration were observed at room temperature and atmospheric pressure. As shown in Figures 2a and 2b, the wavenumbers of the R₁ and R₂ lines decreased with increasing Cr₂O₃ content up to 0.3 wt%, whereas a reversal of this trend occurred at Cr₂O₃ contents greater than 0.3 wt%. The latter observation might be attributed to the fact that the ionic radius of Cr³⁺ is larger than that of Al³⁺. The behavior at Cr₂O₃ contents below approximately 0.3 wt% is not fully understood,

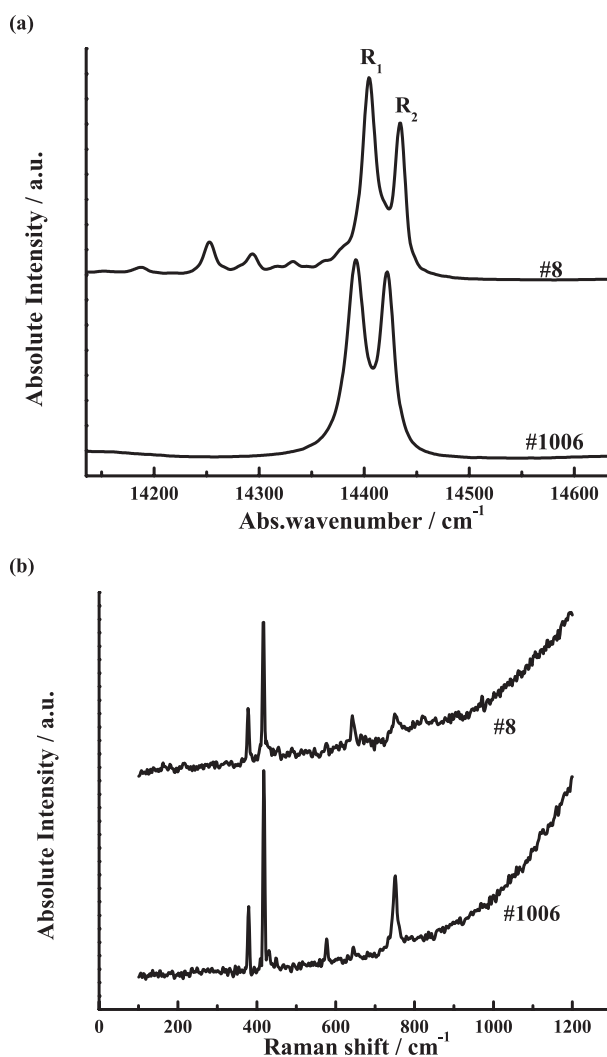


FIGURE 1. (a) Fluorescence spectra of rubies at 298 K and atmospheric pressure, and (b) Raman spectra of rubies at room temperature and atmospheric pressure.

TABLE 1. Weight percent of major and trace elements in the ruby samples

E	1006	4	3	2	5	7	8
Cr ₂ O ₃	0.022 ^a	0.068	0.211	0.279	0.556	1.221	1.676
Fe ₂ O ₃	–	0.002	0.001	0.002	0.011	0.024	0.004
TiO ₂	–	0.002	0.005	0.003	0.005	0.039	0.043
NiO	–	0.006	0.006	0.001	0.007	0.004	0.011
MnO	–	0.008	0.012	0.002	0.015	0.005	0.000
SiO ₂	–	0.012	0.096	0.016	0.016	0.017	0.033
Na ₂ O	–	0.000	0.019	0.008	0.002	0.001	0.000
MgO	–	0.000	0.000	0.000	0.013	0.001	0.000
CaO	–	0.003	0.001	0.000	0.010	0.003	0.000
K ₂ O	–	0.004	0.003	0.010	0.011	0.003	0.004
Al ₂ O ₃	–	99.796	98.541	99.524	98.737	97.122	98.029
Total	–	99.904	98.895	99.845	99.396	98.440	99.800

^a Cr₂O₃ wt% of sample 1006 was measured by AAS, and the other data were measured by electron microprobe.

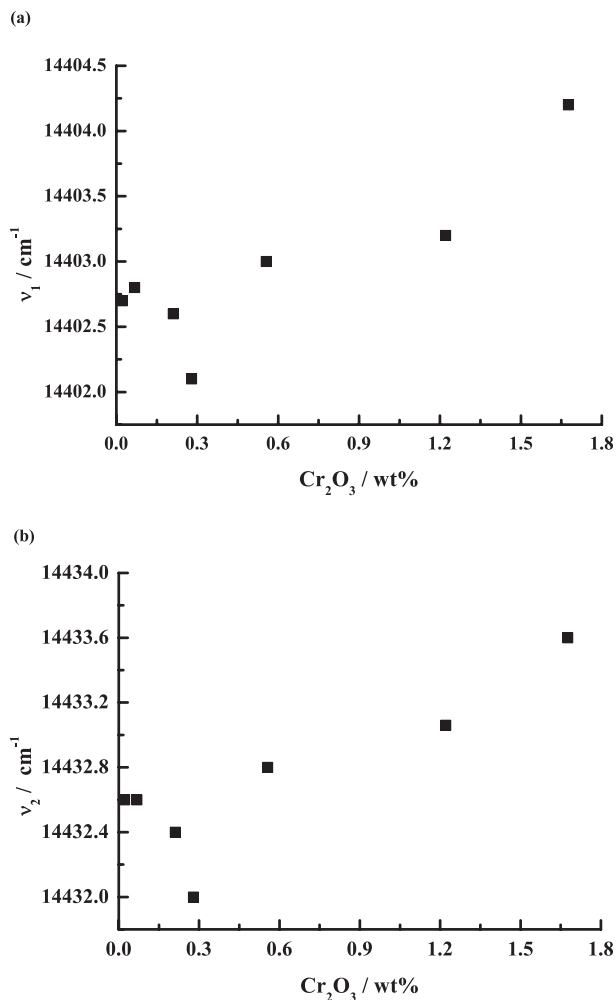


FIGURE 2. Wavenumber values of R lines at room temperature and atmospheric pressure vs. Cr₂O₃ contents in ruby samples, (a) line R₁ and (b) line R₂.

but it might be related to the internal stress that commonly remains in ruby samples because we did not attempt to eliminate the residual stress in our samples before making the fluorescence measurements.

From 300 to 600 K and at atmospheric pressure, the R lines red-shifted linearly with increasing temperature. The relationship between the slope of the R₁ shift with temperature and Cr₂O₃ content is shown in Figure 3a. The absolute values of the slopes decrease with increasing Cr₂O₃ content. The corresponding relationship for R₂ is shown in Figure 3b. In this case, the absolute values of the slopes of the wavenumber shift with temperature also decrease with increasing Cr₂O₃ content below 1.2 wt% content of Cr₂O₃ but recover at higher contents.

Ragan et al. (1992) observed slopes of the R₁ and R₂ shifts with temperature of -0.158 and -0.162 cm⁻¹/K from 300–600 K, respectively, with an unknown Cr³⁺ concentration. They attributed the discrepancy between their results and those of other researchers (-0.14 cm⁻¹/K for R₁ measured by Barnett et al. 1973; -0.153 cm⁻¹/K for R₁ by Yen and Nicol 1992) to the

different methods used to determine the peak positions in the spectra fitting. Spectrum fitting to a double Lorentzian line can allow us to accurately separate the R₁ and R₂ components from overlapping R lines and thereby obtain precise line positions, while obtaining the peak positions by eye (as in Barnett et al. 1973 and Yen and Nicol 1992) will give a R₁ position that does not shift as fast as it should because at high temperatures, the R₁ and R₂ lines overlap and yield a visual R₁ peak that is located at a higher frequency than the line's true resonant frequency. However, significant differences are still present in the slopes of the R line shift among the samples in this study (see Table 2 and Figs. 3a and 3b) even though the wavenumber positions of the R lines were obtained by fitting the spectrum to a double Lorentzian line using high-precision software. Therefore, the discrepancies in the slopes of the R line shift with temperature between various studies cannot be fully explained by the difference in the methods of determining the peak positions. We believe that the major factor was the difference in the Cr³⁺ concentrations in the ruby samples used in this study. The mechanism is discussed in a subsequent section. The anomalous slope of R₂ in sample nos. 1006 and 8 might be attributed to the crystal orientation (Shen and Gupta 1993). The relative intensity of R₁ and R₂ can reflect the crystal orientations in the rubies to some extent. The shifts of the slopes of the R₂ lines with temperature were more closely related to the intensity ratios of R₂ and R₁ (I_2/I_1) (see Figs. 3c and 3d), which is consistent with the greater dependence on the crystal orientation of the R₂ line shift than the R₁ line shift (Shen and Gupta 1993). Moreover, of all the samples, sample nos. 1006 and 8 had the higher I_2/I_1 value (Table 2). In sample nos. 1006 and 8, the fast shift of the R₂ line indicates that the crystal orientation might be closer to the crystal's *c* axis. However, the anomalous fast shift of the R₁ line in sample no. 1006 might be attributed to the lower Cr³⁺ concentration, the crystal orientation and the internal stress.

In the high-pressure DAC experiments (0–2.0 GPa), we found no significant pressure difference in the cell when we used the ruby samples with different Cr₂O₃ contents as pressure calibrants. Figure 4 shows the differences between the pressure that was measured using sample no. 5 and used as the reference pressure in our high-pressure experiments and the pressures measured using the other ruby samples with different Cr₂O₃ contents. All of the differences between the reference pressure and the other measured pressures are within ± 50 MPa, which is a commonly used uncertainty for pressure calibrations when rubies are used as a pressure calibrant in hydrostatic DACs below 2 GPa (Schmidt and Ziemann 2000).

Additional discussion of the impact of Cr³⁺ concentration on the R line shift

Temperature and pressure both have significant impacts on the red-shift of R lines due to the Cr³⁺ doping in rubies. In this study, we found that the Cr³⁺ concentration in a ruby also has an important impact on shift of the R lines. This impact can be summarized as a decrease of the (dv/dT) value of the R lines and a blue-shifting of the R lines with increasing Cr³⁺ concentration in a ruby.

McCumber and Sturge (1963) theoretically interpreted the shift of the R₁ line with temperature. Based on Equation 3a of

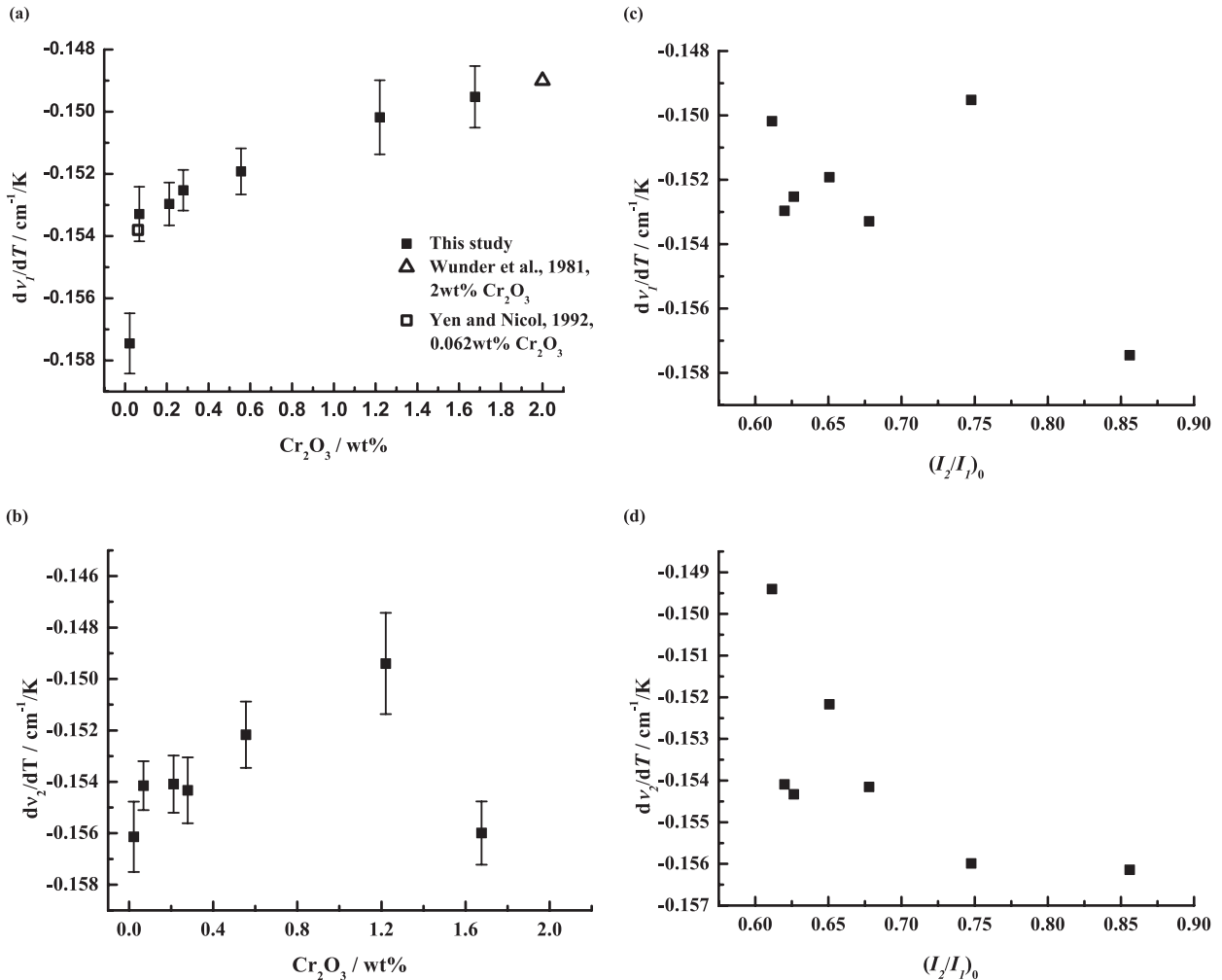


FIGURE 3. Slopes of the wavenumber shift of (a) line R₁ and (b) line R₂ with temperature at atmospheric pressure vs. the Cr₂O₃ contents of different ruby samples, and slopes of the wavenumber shifts of (c) line R₁ and (d) line R₂ with temperature vs. the relative intensity ratios of R₂ to R₁ for different ruby samples at room temperature and atmospheric pressure.

TABLE 2. Relative intensity ratios of R₂ to R₁ at room temperature and atmospheric pressure [(I₂/I₁)₀] and the slopes of the wavenumber shifts of R₁ and R₂ with temperature (dv₁/dT, dv₂/dT) at atmospheric pressure for ruby samples with different Cr₂O₃ contents

Sample no.	Cr ₂ O ₃ (wt%)	(I ₂ /I ₁) ₀	dv ₁ /dT(cm ⁻¹ /K ⁻¹)	dv ₂ /dT(cm ⁻¹ /K ⁻¹)
1006	0.022	0.856 ± 0.003	-0.1574 ± 0.0011	-0.1561 ± 0.0015
4	0.068	0.678 ± 0.011	-0.1533 ± 0.0010	-0.1542 ± 0.0010
3	0.211	0.620 ± 0.012	-0.1530 ± 0.0008	-0.1541 ± 0.0012
2	0.279	0.626 ± 0.007	-0.1525 ± 0.0007	-0.1543 ± 0.0014
5	0.556	0.651 ± 0.009	-0.1519 ± 0.0008	-0.1522 ± 0.0014
7	1.221	0.611 ± 0.001	-0.1501 ± 0.0012	-0.1494 ± 0.0021
8	1.676	0.748 ± 0.005	-0.1495 ± 0.0011	-0.1560 ± 0.0013

McCumber and Sturge, we calculated the derivative of the wavenumber of the R₁ line with respect to temperature as follows,

$$\frac{dv_1(T)}{dT} = a \cdot \left[4 \times \frac{T^3}{T_D} \int_0^{T_D/T} dx \frac{x^3}{e^x - 1} - \frac{1}{T(e^{T_D/T} - 1)^2} \right] \quad (1)$$

where a is the electron-phonon coupling constant, and T_D is the effective Debye temperature. McCumber and Sturge (1963) found that using $a = -400$ cm⁻¹ and $T_D = 760$ K provided a good

fit to the experimental results for 0–700 K. However, Yen and Nicol (1992) found that $a = 400$ cm⁻¹ gives good results for this temperature range. Table 3 shows the values of the constant a that provided the best fits to the measurement results in this study. The rates of the wavenumber shift of the R lines with temperature are closely related to the electron-phonon coupling constant, and the electron-phonon coupling constant a decreases monotonously with increasing Cr³⁺ concentration. According to McCumber and Sturge (1963), the electron-phonon coupling constant a measures the probability of the scattering of phonons from the 3d electrons of Cr³⁺; the larger the value of a , the smaller the probability of scattering. In our case, an increase of the Cr³⁺ concentration in the ruby samples indicates an increase of the density of the scattering center, Cr³⁺, for the phonon. As a result, the probability of scattering would increase, and the value of the phonon-electron coupling constant a decreases with increasing Cr³⁺ concentration. Therefore, our experimental results are consistent with the theoretical model of McCumber and Sturge (1963) of the impact of Cr³⁺ concentration on the value of (dv/dT) of R lines.

To theoretically explain the blue-shift of ruby R lines with increasing Cr³⁺ concentration, we used the first-principle calculation method and conducted a series of calculations of the electronic density of state (DOS) of the Cr³⁺ 3d band for rubies with different Cr³⁺ concentrations at room temperature and atmospheric pressure and at room temperature and 10 GPa. The results (Figs. 5 and 6) show that the peaks of the DOS of the Cr³⁺ 3d electrons are blue-shifted with increasing Cr³⁺ concentration at room temperature and atmospheric pressure and red-shifted with increasing pressure at room temperature and a constant Cr³⁺ concentration. Moreover, with increasing Cr³⁺ concentration at room temperature, the amplitude of the pressure-induced red-shift of the DOS peaks increased when the pressure increased from atmospheric pressure to 10 GPa. Because the red-shift of the DOS peaks of the Cr³⁺ 3d electrons with increasing pressure is a well-known mechanism for the red-shift of ruby R lines with pressure (Xie 2004), the blue-shift of the DOS peaks of the Cr³⁺ 3d electrons with increasing Cr³⁺ concentration should also be the mechanism for the blue-shift of the ruby R lines with increasing Cr³⁺ concentration. This behavior was observed from the experimental results in this study.

The analysis presented above indicates that the Cr³⁺ concentration might have a significant influence on the R line shift of rubies in addition to the important factors of temperature and pressure. It is possible that with increasing Cr³⁺ concentration, there could be increasingly important coupling effects of the influences of temperature, pressure, and Cr³⁺ concentration on the ruby R line shift because the Cr³⁺-Cr³⁺ interactions in the ruby lattice would become stronger (Ohnishi and Sugano 1982; Winter et al. 1990).

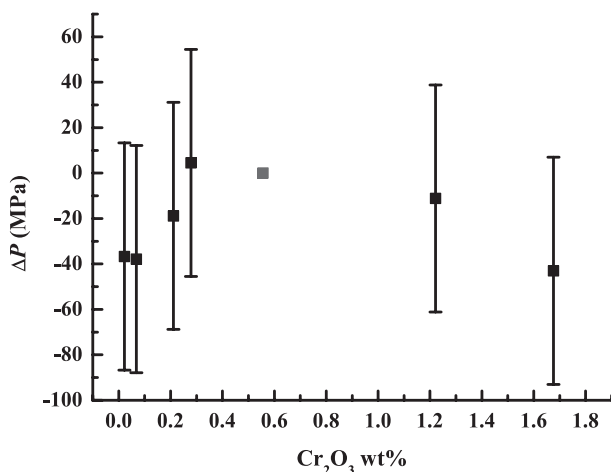


FIGURE 4. Pressure differences between the reference pressure calibrated using ruby sample 5 and those calibrated using the other ruby samples with different Cr₂O₃ contents at 2.0 GPa and room temperature.

TABLE 3. Calculated values of the electron-phonon coupling constant *a* for ruby samples with different contents of Cr₂O₃ (*T_D* = 760 K, *T* = 298.15 K)

Sample no.	1006	4	3	2	5	7	8
Cr ₂ O ₃ (wt%)	0.022	0.068	0.211	0.279	0.556	1.221	1.676
<i>a</i> (cm ⁻¹)	257.2 ± 1.6	250.4 ± 1.5	250.7 ± 1.1	250.7 ± 1.0	248.2 ± 1.1	245.4 ± 1.8	244.3 ± 1.6

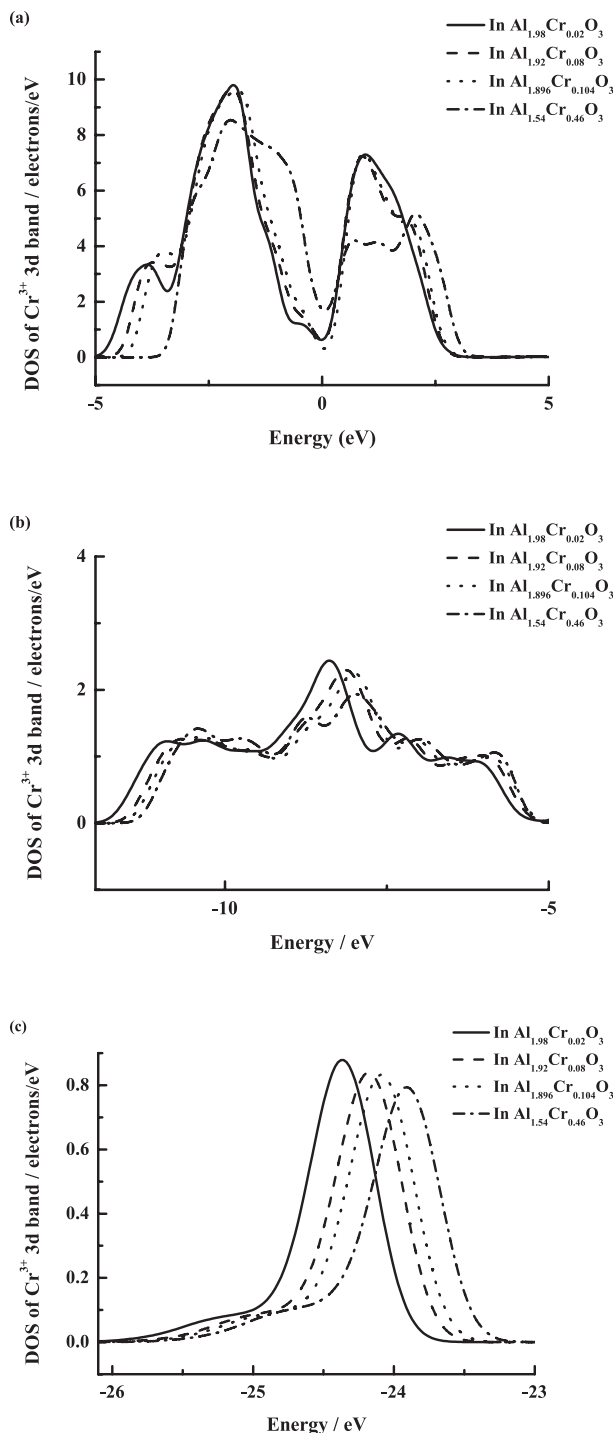


FIGURE 5. Electronic densities of state (DOS) of the Cr³⁺ 3d band in rubies with different Cr₂O₃ contents at room temperature and atmospheric pressure.

Full-width at half maximum (FWHM) of the R lines

The full-width at half maximum of the R₁ line (FWHM₁) at atmospheric pressure and temperature increased significantly with increasing Cr³⁺ concentration, whereas the full-width at half maximum of the R₂ line (FWHM₂) increased moderately (Fig. 7). By linear fits to the experimental data for the R₁ and R₂ lines, we obtained FWHM₁(cm⁻¹) = 11.44348 + 2.33563 × Cr₂O₃ (wt%) with a *r*² value of 0.9978 and FWHM₂ (cm⁻¹) = 8.94403 + 1.1267 × Cr₂O₃ (wt%) with a *r*² value of 0.9986. In contrast, Ragan et al. (1992) reported that the FWHM values of the R lines of rubies that contained 0.12% and 0.5% Cr³⁺ were nearly identical. Theoretically, if two 3d electrons are located in the same type of orbit but belong to two different Cr³⁺ in the ruby lattice, there is always a slight difference in their energy levels due to subtle differences in the electromagnetic environments in which the two Cr³⁺ are located. The difference in energy level changes the energy level into an energy band. With increasing Cr³⁺ concentration in rubies, the energy bands of both the ground states and the excited states of the 3d electrons of Cr³⁺ would widen, and the FWHMs of the ruby R lines that originate from the excitation of 3d electrons from their respective ground states and the subsequent de-excitation

from their corresponding excitation states of Cr³⁺ would also widen. As shown in Figure 7, both FWHM₁ and FWHM₂ show significant linear increases with Cr³⁺ concentration in the range of 0.022–1.67 wt%. Our experimental results are consistent with the theoretical analysis presented above.

At high temperatures and ambient pressure, FWHM₁ increased with temperature from 298–600 K (Fig. 8). These results are consistent with common knowledge. However, two interesting phenomena in our results are worth noting. First, the increasing width of the FWHMs of the R lines with increasing Cr³⁺ concentration observed at room temperature (Fig. 7) was also observed for the R₁ line at higher temperatures. Second, the positive dependence of FWHM₁ on temperature became stronger with increasing temperature.

Relative intensity ratios of R₂ to R₁ (I₂/I₁)

Similar to the results described above, the relative intensities of the R₁ and R₂ lines of all of the ruby samples in this study decreased with increasing temperature at atmospheric pressure. However, the relative intensity of the R₂ line (I₂) decreased more slowly than that of the R₁ line (I₁) at temperatures from 100 K

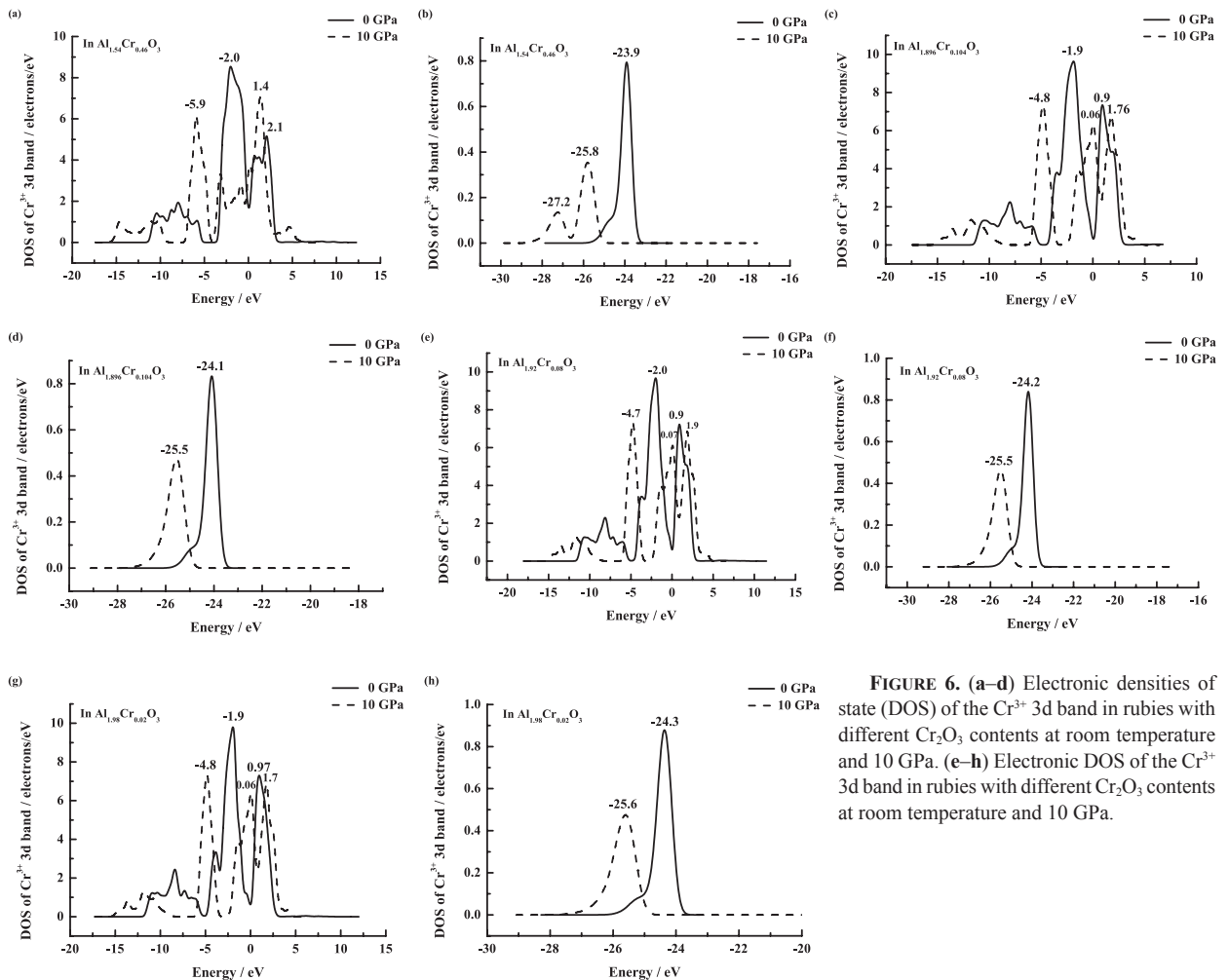


FIGURE 6. (a–d) Electronic densities of state (DOS) of the Cr³⁺ 3d band in rubies with different Cr₂O₃ contents at room temperature and 10 GPa. (e–h) Electronic DOS of the Cr³⁺ 3d band in rubies with different Cr₂O₃ contents at room temperature and 10 GPa.

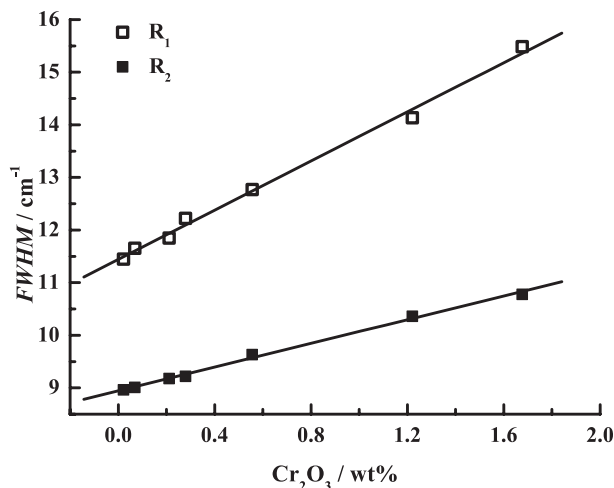


FIGURE 7. Variations of the full-width at half maximum (FWHM) of ruby R lines with Cr₂O₃ contents in different ruby samples at atmospheric pressure and room temperature.

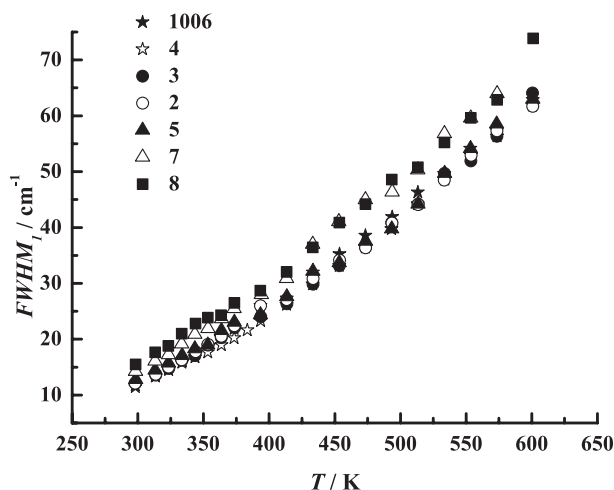


FIGURE 8. Variations of the full-width at half maximum of the R₁ line (FWHM₁) of different ruby samples at atmospheric pressure and a temperature range of 298–600 K.

to approximately 298 K and subsequently decreased faster than I_1 until 600 K, which indicates a significant temperature dependence of I_2/I_1 (Fig. 9a¹). Moreover, the maximum I_2/I_1 values, $(I_2/I_1)_{\max}$, occurred at different temperatures in samples with different Cr₂O₃ contents, and the values of $(I_2/I_1)_{\max}$ and I_2/I_1 at 298 K, i.e., $(I_2/I_1)_0$, were both related to the Cr₂O₃ contents in the samples. As shown in Figure 9b¹, the temperatures that correspond to the values of $(I_2/I_1)_{\max}$ were inversely related to the Cr₂O₃ content. However, it is interesting to note that the relationship between $(I_2/I_1)_{\max}$ and the Cr₂O₃ content was weaker than that between $(I_2/I_1)_0$ and the Cr₂O₃ content at atmospheric pressure. By further

linear fitting, we obtained a relationship between $(I_2/I_1)_{\max}$ and $(I_2/I_1)_0$, which can be expressed as $(I_2/I_1)_{\max} = -0.02036 + 1.04067 \times (I_2/I_1)_0$ with a r^2 value of 0.997 (Fig. 9c¹).

IMPLICATIONS

Pressure calibration is of primary importance for high-pressure experiments. Ruby is the most commonly used pressure calibrant, especially in high-pressure DAC experiments. Temperature corrections in ruby pressure calibrations are especially important at elevated temperatures. The results of this study show that the wavenumber shifts of ruby R lines are related not only to variations of pressure and temperature but also to variations in the Cr³⁺ concentrations of the rubies. Moreover, the three influential factors, temperature, pressure, and Cr³⁺ concentration, have important coupled effects on the wavenumber shifts of the ruby R lines. At room temperature and pressures of 0–2.0 GPa, the results of our DAC experiments show that the differences in the cell pressures calibrated by the ruby samples with different Cr³⁺ concentrations were less than ± 50 MPa, which is a commonly accepted pressure calibration uncertainty for a ruby calibrant in hydrostatic DACs below 2.0 GPa (Schmidt and Ziemann 2000). However, this does not mean that the differences would be within ± 50 MPa at higher temperatures and/or pressures. For example, if we conduct a heating DAC experiment from 300 to 600 K and calibrate the temperature or pressure using the temperature shift rates of the R₁ line wavenumber of sample nos. 1006 and 8 (Table 2), the maximum temperature and pressure differences would be 16 K and 315 MPa, respectively. We conclude that before conducting a DAC experiment, it is important to know the dependence of the ruby R line shift on the temperature, pressure, and Cr³⁺ concentration if rubies are used as the temperature or pressure calibrant. The precision of the ruby temperature or pressure calibration could be improved significantly if these dependences are known in detail. However, a large number of experiments at higher pressures and/or temperatures should be conducted in the future to completely resolve the complicated coupled effects of temperature, pressure, and Cr³⁺ concentration on the wavenumber shifts of the R lines of rubies.

ACKNOWLEDGMENTS

We thank Lin-gun Liu for his help during the research and comments, and the associated editor Jennifer Kung, the reviewer Robert Mayanovic and the anonymous reviewer for their comments to improve the paper. This research was supported by the “135” Program, Institute of Geochemistry, CAS.

REFERENCES CITED

- Angel, R.J., Bujak, M., Zhao, J., Gatta, G.D., and Jacobsen, S.D. (2007) Effective hydrostatic limits of pressure media for high-pressure crystallographic studies. *Journal of Applied Crystallography*, 40, 26–32.
- Barnett, J.D., Block, S., and Piermarini, G.J. (1973) An optical fluorescence system for quantitative pressure measurement in the diamond-anvil cell. *Review of Scientific Instruments*, 44, 1–9.
- Chou, I.M. (2003) Hydrothermal diamond-anvil cell: application to studies of geologic fluids. *Acta Petrologica Sinica*, 19, 213–220.
- Forman, R.A., Piermarini, G.J., Barnett, J.D., and Block, S. (1972) Pressure measurement made by the utilization of ruby sharp-line luminescence. *Science*, 176, 284–285.
- Kokhanenko, P.N., and Antipov, A.B. (1969) Possible determination of the emission wavelength of active ruby from its temperature. II. *Russian Physics Journal*, 12, 37–40.
- Goncharov, A.F., Zaug, J.M., and Crowhurst, J.C. (2005) Optical calibration of pressure sensors for high pressures and temperatures. *Journal of Applied Physics*, 97, 094917.
- Mao, H.K., Xu, J., and Bell, P.M. (1986) Calibration of the ruby pressure gauge to

¹ Deposit item AM-15-75110, Figure 9. Deposit items are stored on the MSA web site and available via the American Mineralogist Table of Contents. Find the article in the table of contents at GSW (ammin.geoscienceworld.org) or MSA (www.minsocam.org), and then click on the deposit link.

- 800 kbar under quasi-hydrostatic conditions. *Journal of Geophysical Research*, 91, 4673–4676.
- McCumber, D.E., and Sturge, M.D. (1963) Linewidth and temperature shift of the R lines in ruby. *Journal of Applied Physics*, 34, 1682–1684.
- Ohnishi, S., and Sugano, S. (1982) Theoretical studies of high-pressure effects on optical properties of ruby. *Japanese Journal of Applied Physics*, 21, L309–L311.
- Perdew, J.P., Burke, K., and Ernzerhof, M. (1996) Generalized gradient approximation made simple. *Physical Review Letters*, 77, 3865–3868.
- Ragan, D.D., Gustavsen, R., and Schiferl, D. (1992) Calibration of the ruby R₁ and R₂ fluorescence shifts as a function of temperature from 0 to 600K. *Journal of Applied Physics*, 72, 5539–5544.
- Schmidt, C., and Ziemann, M.A. (2000) In-situ Raman spectroscopy of quartz: A pressure sensor for hydrothermal diamond-anvil cell experiments at elevated temperatures. *American Mineralogist*, 85, 1725–1734.
- Shen, X.A., and Gupta, Y.M. (1993) Effect of crystal orientation on ruby R-line shifts under shock compression and tension. *Physical Review B*, 48, 2929–2940.
- Weinstein, B.A. (1986) Ruby thermometer for cryobaric diamond-anvil cell. *Review of Scientific Instruments*, 57, 910–913.
- Winter, N.W., Ross, M., and Pitzer, R.M. (1990) Calculation of the pressure shifts of the quartet states of ruby. *Journal of Physical Chemistry*, 94, 1172–1174.
- Wunder, S.L., and Schoen, P.E. (1981) Pressure measurement at high temperatures in the diamond anvil cell. *Journal of Applied Physics*, 52, 3772–3775.
- Xie, Y.L. (2004) High temperature high pressure study of the R1 ruby fluorescence line, 41–46 p. Master thesis, Jilin University, Changchun.
- Yamaoka, S., Shimomura, O., and Fukunaga, O. (1980) Simultaneous measurements of temperature and pressure by the ruby fluorescence line. *Proceedings of the Japan Academy. Ser. B: Physical and Biological Sciences*, 56, 103–107.
- Yen, J., and Nicol, M. (1992) Temperature dependence of the ruby luminescence method for measuring high pressure. *Journal of Applied Physics*, 72, 5535–5538.

MANUSCRIPT RECEIVED JUNE 26, 2014
MANUSCRIPT ACCEPTED JANUARY 20, 2015
MANUSCRIPT HANDLED BY JENNIFER KUNG